

Geophysical Research Letters®



RESEARCH LETTER

10.1029/2023GL105889

Key Points:

- Heterogeneous chemistry on solid alumina particles is highly uncertain and depends strongly on the partitioning of acids onto the surface
- The reaction rate of ClONO₂ with HCl on alumina particles is uncertain by up to two orders of magnitude under stratospheric conditions
- Injection of 5 Mt/yr of alumina particles could double global ozone reductions compared to chlorofluorocarbons in the late 1990s

Supporting Information:

Supporting Information may be found in the online version of this article.

Correspondence to:

S. Vattioni,
sandro.vattioni@env.ethz.ch

Citation:

Vattioni, S., Luo, B., Feinberg, A., Stenke, A., Vockenhuber, C., Weber, R., et al. (2023). Chemical impact of stratospheric alumina particle injection for solar radiation modification and related uncertainties. *Geophysical Research Letters*, 50, e2023GL105889. <https://doi.org/10.1029/2023GL105889>

Received 18 AUG 2023

Accepted 18 NOV 2023

Author Contributions:







Conceptualization: Sando Vattioni, Beiping Luo, Frank Keutsch, Thomas Peter

Formal analysis: Christof Vockenhuber, Rahel Weber

Funding acquisition: Sando Vattioni, Markus Ammann, Frank Keutsch, Thomas Peter, Gabriel Chiodo

Investigation: Sando Vattioni, Beiping Luo, Christof Vockenhuber, Rahel Weber, John A. Dykema

Chemical Impact of Stratospheric Alumina Particle Injection for Solar Radiation Modification and Related Uncertainties

Sando Vattioni^{1,2} , Beiping Luo¹, Aryeh Feinberg^{1,3,4} , Andrea Stenke^{1,3,5} , Christof Vockenhuber⁶ , Rahel Weber^{1,2}, John A. Dykema² , Ulrich K. Krieger¹ , Markus Ammann⁷, Frank Keutsch^{2,8,9} , Thomas Peter¹, and Gabriel Chiodo¹ 

¹Institute for Atmospheric and Climate Science, ETH Zürich, Zürich, Switzerland, ²John A. Paulson School of Engineering and Applied Sciences, Harvard University, Cambridge, MA, USA, ³Institute of Biogeochemistry and Pollutant Dynamics, ETH Zürich, Zürich, Switzerland, ⁴Now at Institute for Data, Systems, and Society, Massachusetts Institute of Technology, Cambridge, MA, USA, ⁵Eawag, Swiss Federal Institute of Aquatic Science and Technology, Dübendorf, Switzerland, ⁶Laboratory of Ion Beam Physics, ETH Zürich, Zürich, Switzerland, ⁷Laboratory of Atmospheric Chemistry, Paul Scherrer Institute, Villigen, Switzerland, ⁸Department of Chemistry and Chemical Biology, Harvard University, Cambridge, MA, USA, ⁹Department of Earth and Planetary Sciences, Harvard University, Cambridge, MA, USA

Abstract Compared to stratospheric SO₂ injection for climate intervention, alumina particle injection could reduce stratospheric warming and associated adverse impacts. However, heterogeneous chemistry on alumina particles, especially chlorine activation via ClONO₂ + HCl $\xrightarrow{\text{surf}}$ Cl₂ + HNO₃, is poorly constrained under stratospheric conditions, such as low temperature and humidity. This study quantifies the uncertainty in modeling the ozone response to alumina injection. We show that extrapolating the limited experimental data for ClONO₂ + HCl to stratospheric conditions leads to uncertainties in heterogeneous reaction rates of almost two orders of magnitude. Implementation of injection of 5 Mt/yr of particles with 240 nm radius in an aerosol-chemistry-climate model shows that resulting global total ozone depletions range between negligible and as large as 9%, that is more than twice the loss caused by chlorofluorocarbons, depending on assumptions on the degree of dissociation and interaction of the acids HCl, HNO₃, and H₂SO₄ on the alumina surface.

Plain Language Summary Global warming caused by increasing greenhouse gases could be temporarily reduced by introducing aerosol particles into the stratosphere. The most frequently studied approach to climate intervention uses H₂SO₄-H₂O aerosols, which, however, could result in undesirably strong warming of the stratosphere and significant ozone depletion. This might be improved by injecting solid particles, for example, made of aluminum oxide. However, here we show that the extremely limited availability of experimental studies on heterogeneous chemistry on alumina under the influence of stratospheric concentrations of HCl, HNO₃, H₂SO₄, and H₂O leads to large uncertainties in the impact of alumina injection on stratospheric ozone. In order to quantify these uncertainties, we integrated the currently available knowledge about the most important heterogeneous reaction ClONO₂ + HCl $\xrightarrow{\text{surf}}$ Cl₂ + HNO₃ into an aerosol-chemistry-climate model. We conclude that the uncertainty in the resulting heterogeneous reaction rate is more than two orders of magnitude depending on the partitioning of HCl, H₂SO₄, and HNO₃ on the alumina surface. This could lead to global ozone column depletion ranging between almost negligible and up to 9%, which would be more than twice as much as the ozone loss caused by chlorofluorocarbons in the late 1990s.

1. Introduction

Since preindustrial times, atmospheric greenhouse gas (GHG) concentrations have risen to levels never before experienced by humankind, with negative consequences for the environment and society (Arias et al., 2021; Jouzel, 2013). Even if society succeeded in rapidly ceasing emissions, global warming and its impacts would linger for millennia as carbon dioxide removal techniques may not prove efficient or may not be scaled up fast enough (Clark et al., 2016; NRC, 2015). These prospects have motivated proposals for stratospheric aerosol injection (SAI) as an affordable intervention strategy that could provide immediate cooling to counteract some of the impacts of climate change (Budyko, 1977; Crutzen, 2006). SAI could potentially serve as a temporary supplement to measures that actually address the cause of climate change, such as GHG mitigation and adaptation, until society finds solutions on how to remove long-lived GHGs from the atmosphere (Keith & MacMartin, 2015;

© 2023. The Authors.

This is an open access article under the terms of the [Creative Commons Attribution-NonCommercial-NoDerivs License](https://creativecommons.org/licenses/by-nc-nd/4.0/), which permits use and distribution in any medium, provided the original work is properly cited, the use is non-commercial and no modifications or adaptations are made.

Methodology: Sando Vattioni, Beiping Luo, John A. Dykema, Frank Keutsch, Thomas Peter

Project Administration: Thomas Peter, Gabriel Chiodo

Software: Sando Vattioni, Aryeh Feinberg, Andrea Stenke

Supervision: Frank Keutsch, Thomas Peter, Gabriel Chiodo

Validation: Beiping Luo, Aryeh Feinberg, Andrea Stenke

Visualization: Sando Vattioni, Rahel Weber, Thomas Peter

Writing – original draft: Sando Vattioni

Writing – review & editing: Beiping Luo, Aryeh Feinberg, Andrea Stenke, Christof Vockenhuber, Ulrich K. Krieger, Markus Ammann, Frank Keutsch, Thomas Peter, Gabriel Chiodo

MacMartin et al., 2014). It has been proposed that SAI might help to limit global warming to 1.5°C, the target set by the Paris Agreement in 2015 (MacMartin et al., 2018). However, despite potential benefits of SAI there are large uncertainties about risks associated with negative side effects, for example, its impact on stratospheric chemistry (e.g., Robock, 2008).

Until now, most research on SAI has focused on SO₂ as the injected species, motivated by the observed cooling after explosive volcanic eruptions, such as Mt. Pinatubo in 1991 (Bluth et al., 1992; Wilson et al., 1993). Sulfuric acid aerosols are formed after the oxidation of SO₂ in the stratosphere. However, SAI by sulfuric acid aerosols bears several limitations, including optically inefficient aerosol size distributions (Vattioni et al., 2019), stratospheric ozone depletion (Tilmes et al., 2008; Vattioni et al., 2019; Weisenstein et al., 2022), and stratospheric heating (Aquila et al., 2014; Dykema et al., 2016). This has repercussions for global atmospheric dynamics potentially with additional feedbacks on stratospheric chemistry.

Recent studies have shown that the injection of solid particles, such as alumina (Al₂O₃), calcite (CaCO₃) or diamond (C) particles might reduce some of the limitations of sulfuric acid-based SAI (Dykema et al., 2016; Ferraro et al., 2011; Keith et al., 2016; Pope et al., 2012; Weisenstein et al., 2015). In particular, it has been suggested that the optical properties of some of these materials would result in smaller stratospheric heating because of less absorption of infrared radiation and more efficient backscattering of solar radiation per stratospheric aerosol burden than SAI by sulfuric acid aerosols (Dykema et al., 2016). In addition, it has been suggested that solid particles such as alumina or calcite could result in reduced ozone depletion compared to SAI by sulfuric acid aerosols (Keith et al., 2016; Weisenstein et al., 2015; WMO, 2022). Based on these lines of evidence, the IPCC-AR6 inferred that injection of non-sulfate aerosols is likely to result in less stratospheric heating and ozone loss (Arias et al., 2021). However, previous studies are based on simplifying assumptions about particle reactivity under stratospheric conditions, due to lack of experimental data. Therefore, uncertainties remain high regarding SAI of solid particles, especially concerning their impact on stratospheric ozone.

1.1. Aging and Non-Aging Solid Particles

There is only limited knowledge about the physical chemistry of solid particles under stratospheric conditions, especially with respect to temperature (<220 K), relative humidity (<1%), interactions with stratospheric chemical species, and UV irradiation. The various materials under consideration can be divided into two categories. On the one hand, solids such as calcite (CaCO₃) particles that are expected to undergo “chemical aging” during their stratospheric residence time of about 1 year (Dai et al., 2020; Huynh & McNeill, 2021). On the other hand, solids such as alumina (Al₂O₃), which are not expected to undergo significant chemical aging. For example, in the first category, calcite particles could change their composition and crystalline structure upon reaction with the stratospheric acids H₂SO₄, HNO₃ or HCl, which is likely to affect their optical and chemical properties (Keith et al., 2016). In the second category, alumina will likely not react with stratospheric gases, but a thin H₂SO₄-H₂O coating, partially or fully covering the particles, may result from H₂SO₄-H₂O co-condensation and coagulation with stratospheric background aerosol particles (see also Weisenstein et al., 2015). While the inertness of alumina significantly reduces uncertainties of particle evolution under stratospheric conditions compared to solid particles with chemical aging, it is at present uncertain whether “non-aging” particle surfaces may host heterogeneous chemistry of trace gases such as HCl, ClONO₂, HNO₃, and H₂SO₄. The lack of experimental data makes it difficult to quantify surface processes and heterogeneous reactions on solid particles as a function of temperature, relative humidity, and material properties, like hydrophilicity, under stratospheric conditions.

1.2. Experimental Data on Heterogeneous Chemistry on Alumina Particles

Molina et al. (1997) demonstrated that alumina may provide the surface for heterogeneous surface reaction R1, which contributes to stratospheric chlorine activation:



HCl and ClONO₂ are important reservoir species of stratospheric chlorine and nitrogen oxides, ClO_x and NO_x, which destroy ozone catalytically. Thus, solid particles can provide surfaces for heterogeneous chlorine activation reactions, which may result in significant ozone loss (after Cl₂ photolysis). Molina et al. (1997) provide the only experimental study investigating R1 on alumina surfaces at stratospheric temperatures. They performed flow tube

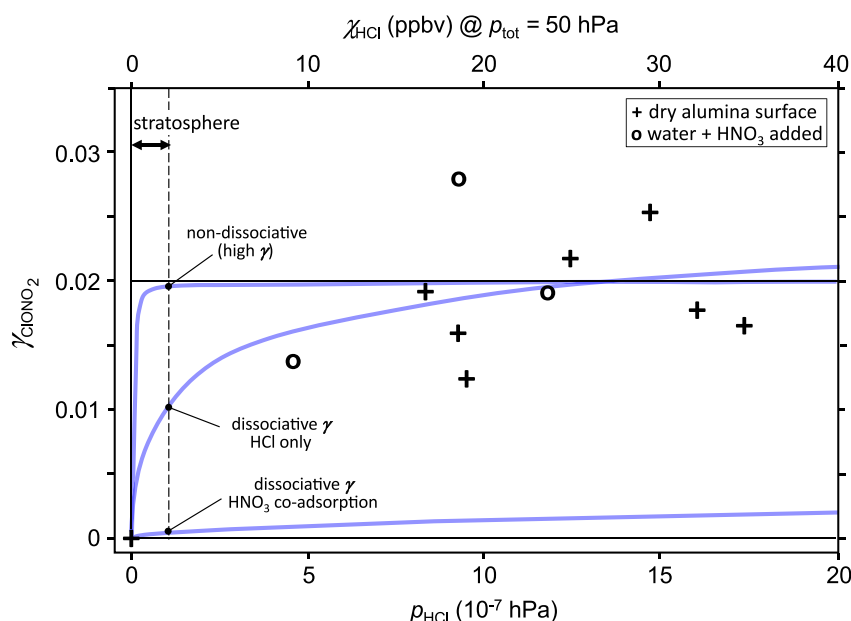


Figure 1. Reaction probability γ_{CIONO_2} for $\text{CIONO}_2 + \text{HCl}$ on alumina measured by Molina et al. (1997) as a function of p_{HCl} (black symbols) in comparison with uptake coefficients calculated from isotherms of adsorption/desorption and reaction rate coefficients (blue curves). Measurements were performed under dry conditions (crosses) or after adding 2.5×10^{-4} hPa water and 4.5×10^{-7} hPa HNO_3 (circles), see Text S1 in Supporting Information S1. The uptake coefficient based on dissociative adsorption of “HCl only” was calculated using $1/\gamma_{\text{CIONO}_2} = 1/\alpha_{\text{CIONO}_2} + 1/(\beta \sqrt{p_{\text{HCl}}})$ with α and β fitted to the data, for HNO_3 co-adsorption using $1/\gamma_{\text{CIONO}_2} = 1/\alpha_{\text{CIONO}_2} + 1/(33 \beta \sqrt{p_{\text{HCl}}})$, and for non-dissociative HCl adsorption using $1/\gamma_{\text{CIONO}_2} = 1/\alpha_{\text{CIONO}_2} + 1/(\beta p_{\text{HCl}})$ with fixed values $\alpha_{\text{CIONO}_2} = 0.02$ and $\beta = 2.7 \times 10^7$ hPa, resulting in a “high” γ_{CIONO_2} of 0.019 at 50 hPa and 1 ppb HCl (see Table S1 in Supporting Information S1). Typical stratospheric values of p_{HCl} are 1×10^{-7} hPa or lower (dashed vertical line). Axis on top shows HCl mixing ratio χ_{HCl} for a total pressure of 50 hPa representative of ~ 20 km altitude in the stratosphere, for reference.

measurements of R1 and found a reaction probability $\gamma_{\text{CIONO}_2} \approx 0.02$ for temperatures ranging from 208 to 223 K and HCl concentrations ranging from 4.5×10^{-7} to 1.7×10^{-6} hPa (corresponding to 9–35 ppb at 50 hPa, i.e., at about 20 km altitude, Figure 1). Their study aimed at quantifying the impact of space shuttle exhaust, which contains alumina, HCl and water (Potter, 1978). Therefore, Molina et al. (1997) used HCl with concentrations one order of magnitude higher than typical stratospheric volume mixing ratios (~ 1 ppb at 50 hPa under present day conditions). Text S1 in Supporting Information S1 provides more details on their measurement conditions. We extrapolate these measured reaction probabilities to HCl partial pressures representative of the present-day stratosphere by using a Langmuir-Hinshelwood molecular description of co-adsorption/desorption and reaction (e.g., Aguzzi & Rossi, 2001; Carslaw & Peter, 1997; Fernandez et al., 2005; Tabazadeh & Turco, 1993). This requires knowledge of the temperature dependent second order rate coefficient of R1 and the Langmuir constants (i.e., the ratio of forward reaction constant for adsorption over backward reaction constant for desorption) for CIONO_2 and HCl on alumina particles, which cannot be directly retrieved from the Molina et al. (1997) measurements. Therefore, extrapolation to typical stratospheric partial pressures of HCl is subject to large uncertainty, which we will quantify in this study.

1.3. Previous Modeling Studies on SAI of Alumina Particles

Using a 2D-aerosol chemistry climate model, Weisenstein et al. (2015) were the first to study alumina particles for SAI. In their scenario, which resulted in the smallest ozone depletion in relation to the achieved radiative forcing, 4 Mt/yr of alumina particles with a radius of 240 nm were injected. This simulation resulted in a globally averaged clear sky shortwave radiative forcing of -1.2 W/m^2 and globally averaged depletion of the total ozone column (TOC) of 3.4% with values of up to 7% over the poles assuming year 2000 concentrations of ozone depleting substances (ODS).

Weisenstein et al. (2015) distinguished between bare alumina particles and alumina particles, which acquired a sulfuric acid coating due to gaseous H_2SO_4 adsorption or coagulation with sulfuric acid particles. They estimated that 70%–92% of the alumina surface area density (SAD) would be H_2SO_4 -coated and applied the same heterogeneous chemistry as for aqueous H_2SO_4 aerosols. Conversely, only 8%–30% of the total resulting SAD increase in the lower stratosphere was treated as bare alumina SAD for **R1** with $\gamma_{\text{ClONO}_2} = 0.02$. Extrapolation to HCl partial pressures was done by scaling γ_{ClONO_2} with the logarithm of the ratio $[\text{HCl}]/[\text{ClONO}_2]$, an ad-hoc assumption which quenches **R1** for very small $[\text{HCl}]$, but is hard to justify physically or in view of Molina et al. (1997) measurements (see also Text S2 in Supporting Information S1).

On aqueous sulfuric acid aerosol and on the H_2SO_4 -coated fraction of the alumina surface, the N_2O_5 hydrolysis **R2**



is the most important heterogeneous reaction. **R2** removes active nitrogen from the NO_x -induced ozone-depletion cycle and, thus, also weakens deactivation of ClO_x via



Therefore, in the present chlorine-rich stratosphere **R2** results in increased ozone destruction, albeit to a lesser degree than the direct chlorine activation via **R1**. The estimates of Weisenstein et al. (2015) are subject to large uncertainties, mainly due to two factors, which both, will be addressed in this paper: (a) how the Molina et al. (1997) measurements of **R1** were extrapolated to present-day stratospheric HCl concentrations and (b) the assumption made on SAD availability of bare versus H_2SO_4 -coated alumina. In reality, the situation is more complex. Bare alumina particles injected into the stratosphere would immediately be subject to adsorption of stratospheric trace gas molecules HNO_3 , $\text{H}_2\text{SO}_{4(\text{g})}$, HCl, ClONO_2 , and coagulation with $\text{H}_2\text{SO}_{4(\text{aq})}$. Except for H_2SO_4 , these gases are present at ppb mixing ratios, so their collision frequency with the surfaces would be sufficient to establish a molecular monolayer within a few minutes. However, this neglects desorption and given the low partial pressure of these gases it is unlikely that the coverage would exceed a small fraction of a monolayer. In contrast, even though H_2SO_4 has mixing ratios several orders of magnitude lower, it is the only trace gas whose vapor pressure is low enough to form a stable aqueous solution. This results in co-condensation of $\text{H}_2\text{SO}_{4(\text{g})}$ and $\text{H}_2\text{O}_{(\text{g})}$ on available surfaces, while other trace gases adsorb and readily desorb again. Assuming an alumina SAD of $3 \mu\text{m}^2/\text{cm}^3$ in the lower stratosphere (Figure S6b in Supporting Information S1), the condensation rate of $\text{H}_2\text{SO}_{4(\text{g})}$ on the particle surface is roughly one monolayer of H_2SO_4 per 2 weeks (Text S3 in Supporting Information S1). In the initial phase after injection, the surface must still be treated as blank alumina with a few adsorbed trace gas molecules, but during the stratospheric residence time the particles could acquire a $\text{H}_2\text{SO}_{4(\text{aq})}$ -coating of nominally ~ 10 nm thickness (Text S3 in Supporting Information S1).

2. Methods

We performed Elastic Recoil Detection Analysis (ERDA, Kottler et al., 2006) experiments to test the assumption of alumina being non-aging under stratospheric conditions. Figure S4 in Supporting Information S1 describes the results and provide evidence that alumina is unlikely to change its composition or crystalline structure under exposures to HNO_3 as in the stratosphere. We further measured the wettability of the alumina surface to determine whether the H_2SO_4 - H_2O condensate of nominally ~ 10 nm thickness on the alumina particles fully wets the surface or tends to contract and form small islands of liquid. Figure S3 in Supporting Information S1 shows that aqueous H_2SO_4 droplets on alumina single crystals have contact angles of around 30° (Corti & Krieger, 2007; McLachlan & Cox, 1975; Thomason & Peter, 2006). If this is also true for the 240-nm particles investigated here, the condensed material would contract and only cover a small fraction of the surface. On the uncovered fraction of the surface HCl can react with ClONO_2 , but might be impaired by the co-adsorbing HNO_3 . Therefore, understanding **R1** on these particle surfaces requires modeling, which we describe subsequently.

2.1. Reactive Uptake on Alumina Surfaces

Heterogeneous reaction rates k can be calculated by

$$k = \frac{\gamma \bar{v} \text{SAD}}{4}, \quad (1)$$

where SAD is the surface area density, \bar{v} is the mean molecular speed of the molecules colliding with the surface and γ is the reaction probability, that is, the probability that such a collision actually results in a reaction. For the reaction $\text{ClONO}_2 + \text{HCl}$, γ_{ClONO_2} depends on the amount of HCl available. SAD is determined by the injection rate and size of the aerosol particles. For a given injection mass, smaller particles result in larger SAD because of the larger surface-to-mass ratio and because of smaller sedimentation velocities.

The reaction probability, γ , of heterogeneous reactions for reactants with low adsorptivity on alumina surfaces, such as HCl and ClONO_2 in R1, can be described for example, by a Eley-Rideal mechanism or a Langmuir-Hinshelwood mechanism for adsorption/desorption and reaction. Some studies found that the Eley-Rideal mechanism is more accurate to represent R1 (Fernandez et al., 2005). However, the Langmuir-Hinshelwood mechanism was also successfully used to describe heterogeneous reactions such as R1 on polar stratospheric clouds (e.g., Aguzzi & Rossi, 2001; Ammann et al., 2013; Burkholder et al., 2020; Carslaw & Peter, 1997; Crowley et al., 2010; Fernandez et al., 2005). In this study we use the Langmuir-Hinshelwood mechanism to extrapolate the measurements of Molina et al. (1997) to stratospheric HCl concentrations (i.e., ~ 1 ppb at 50 hPa). As derived in Text S5 in Supporting Information S1, the reaction probability γ_{ClONO_2} can be described by

$$\frac{1}{\gamma_{\text{ClONO}_2}} = \frac{1}{\alpha_{\text{ClONO}_2}} + \frac{\bar{v} \sigma^2}{4 K_{\text{ClONO}_2} k_B T k^{\text{II}} \theta_{\text{Cl}^-}}, \quad (2)$$

where α_{ClONO_2} is the surface accommodation coefficient of species ClONO_2 on alumina, σ is the surface area per adsorption site, K_X is the Langmuir constant of species X, k^{II} the second order surface reaction rate coefficient of R1, k_B the Boltzmann constant, and T the absolute temperature. Under stratospheric conditions, the fractional surface coverage θ_{Cl^-} depends not only on the HCl partial pressure, but also on the competitive HNO_3 co-adsorption (Text S5 in Supporting Information S1):

$$\theta_{\text{Cl}^-} \approx \frac{K_{\text{HCl}} p_{\text{HCl}}}{\theta_{\text{NO}_3^-}} \approx \frac{K_{\text{HCl}} p_{\text{HCl}}}{\sqrt{K_{\text{HNO}_3} p_{\text{HNO}_3}}} \approx \frac{1}{f} \sqrt{K_{\text{HCl}} p_{\text{HCl}}}, \quad (3)$$

where the first expression, $K_{\text{HCl}} p_{\text{HCl}} / \theta_{\text{NO}_3^-}$, reveals the dissociative nature of adsorption and the competition of HCl and HNO_3 via H^+ -concentration on the surface. In Equation 3, f is the reduction factor by which the adsorption of HCl is diminished due to the presence of HNO_3 relative to a system without HNO_3 interaction. In the absence of measurements on alumina, we have estimated f from a comparison of measurements of the HCl uptake on ice with HNO_3 (Hynes et al., 2002) and without HNO_3 (Zimmermann et al., 2016) and find $f \approx 33$ (Text S5 in Supporting Information S1). In Equations 2 and 3, we combine the unknown quantities K_{ClONO_2} , K_{HCl} , and k^{II} as follows:

$$\beta = \frac{4 K_{\text{ClONO}_2} k_B T k^{\text{II}} \sqrt{K_{\text{HCl}}}}{\bar{v} \sigma^2 f}. \quad (4)$$

Thus:

$$\frac{1}{\gamma_{\text{ClONO}_2}} = \frac{1}{\alpha_{\text{ClONO}_2}} + \frac{1}{\beta \sqrt{p_{\text{HCl}}}}. \quad (5)$$

This allows us to describe the measured γ_{ClONO_2} by treating the unknown quantities α_{ClONO_2} and β as fit parameters. Finally, we use the fit of Equation 5 to Molina et al. (1997) measurements and scale it down by f to take into account the HCl- HNO_3 interaction.

Figure 1 shows Equation 5 (blue curves) fitted to Molina et al. (1997) data (black symbols) as a function of HCl partial pressure. The curve labeled “dissociative γ_{ClONO_2} , HCl only” shows a least squares best fit of Equation 5 to the measurements with $f = 1$ for pure HCl uptake (i.e., HNO_3 and H_2SO_4 absent). The curve labeled “dissociative γ_{ClONO_2} , HNO_3 co-adsorption” is the same, but with $f = 33$ derived from measurements of HCl uptake in competition with HNO_3 on ice. Finally, the curve labeled “non-dissociative, high γ_{ClONO_2} ” assumes HCl molecules not to dissociate on the surface (Carslaw & Peter, 1997), and further assumes a high value of β , to span the full range

of possible γ_{ClONO_2} compatible with the data (Table S1 in Supporting Information S1 also provides examples with medium and low γ_{ClONO_2}).

Besides ClONO_2 and HCl , Molina et al. (1997) also examined the effects of the presence of stratospheric concentrations of H_2O and HNO_3 , but found no measurable change in γ_{ClONO_2} (within the range 0.018–0.022), which is seemingly in contradiction with Equation 3. However, it would be misleading to assume that these two gases have no effect on R1 under present-day stratospheric conditions. Because Molina et al. (1997) applied H_2O and HNO_3 at stratospheric concentrations, but HCl at concentrations more than 10-times higher, the effects of H_2O and HNO_3 were likely dwarfed by the excess of HCl . In addition, the impact of H_2SO_4 was not examined by Molina and coworkers. In summary, trace gases, such as HNO_3 , co-adsorb on the particle surface and H_2SO_4 can condense on it (with H_2O). These acids, besides occupying adsorption sites on the surface, will likely dissociate and lead to a highly acidic environment that reduces the adsorptivity of HCl (Text S5 in Supporting Information S1). Therefore, γ_{ClONO_2} measured by Molina et al. (1997) with no HNO_3 or too little HNO_3 is likely an overestimate compared to stratospheric conditions.

All curves in Figure 1 are plausible representations of the γ_{ClONO_2} measured by Molina et al. (1997). Obviously, the measured data do not help constraining γ_{ClONO_2} for low stratospheric p_{HCl} , where the Langmuir adsorption isotherms are in the linear, unsaturated regime. At 1 ppb HCl , γ_{ClONO_2} can be as large as 0.019 (“non-dissociative high γ ”) or as small as 0.0003 (γ with HNO_3 co-adsorption and dissociation), a ratio of almost two orders of magnitude (Figure 1, Table S1 in Supporting Information S1).

2.2. Aerosol-Chemistry-Climate Model Description

We determined the stratospheric ozone response to injection of alumina particles by means of the aerosol-chemistry-climate model SOCOL-AERv2 (Feinberg et al., 2019), which allows to represent all relevant aspects of stratospheric chemistry and dynamics. Its dynamical core is ECHAM5.4 (Roeckner et al., 2003), which is interactively coupled to the chemistry module MEZON (Egorova et al., 2003; Rozanov et al., 2001; Stenke et al., 2013) and the sectional aerosol module AER (Sheng et al., 2015; Weisenstein et al., 1997). SOCOL-AERv2 employs a T42 horizontal resolution (i.e., 310×310 km at the equator) and 39 vertical sigma pressure levels up to 0.01 hPa (i.e., ~ 80 km). It represents stratospheric chemistry with 40 sulfuric acid aerosol mass bins and 89 gas phase species including all relevant chlorine, nitrogen, carbon, bromine, oxygen, hydrogen, and sulfur species which interact with each other through 16 heterogeneous, 58 photolysis, and 160 gas phase reactions. The aerosols, the chemistry, and the dynamics are fully interactive with each other allowing for accurate representation of stratospheric dynamics and chemistry (e.g., Brodowsky et al., 2021; Friedel & Chiodo, 2022).

The aerosol module in SOCOL-AERv2 was extended to include tracers for spherical monomers and agglomerates of alumina particles, assuming a density of 3.95 g/cm^3 . Ten prognostic variables (mass bins) were integrated to represent the injection of monomers with 240 and 80 nm radius and their agglomeration, while assuming mass doubling between subsequent mass bins. Self-coagulation of alumina particles follows the description of Weisenstein et al. (2015). SAD is calculated as the sum of the area of the number of monomers per agglomerate assuming the contact between single monomers within an agglomerate to be infinitely small. Their sedimentation as well as wet and dry deposition in the troposphere is treated the same way as for sulfuric acid aerosols (Feinberg et al., 2019). Scattering and absorption of radiation by alumina particles and stratospheric sulfuric acid aerosols were not accounted for in this study to isolate the impact of heterogeneous chemistry on alumina particle surfaces. The alumina particles are assumed not to interact with sulfuric acid aerosols except in the scenarios labeled “ H_2SO_4 coating.” In these scenarios, alumina particles acquire a sulfuric acid coating through coagulation with sulfuric acid aerosols and H_2SO_4 - H_2O co-condensation (following Weisenstein et al., 2015), and the heterogeneous chemistry on the entire resulting SAD is assumed to be identical to sulfuric acid aerosols (see Sheng et al., 2015).

2.3. Modeling Scenarios

Each alumina injection scenario (Table S1 in Supporting Information S1) assumes an emission of 5 Mt/yr of Al_2O_3 particles between 30°N and 30°S at all longitudes at the 54 hPa level (~ 20 km altitude). Particle radius is 240 nm (reference case) or 80 nm (sensitivity analysis). In Weisenstein et al. (2015) injections at particle radius of 240 nm resulted in the best tradeoff between global cooling and ozone depletion per injected aerosol mass (see

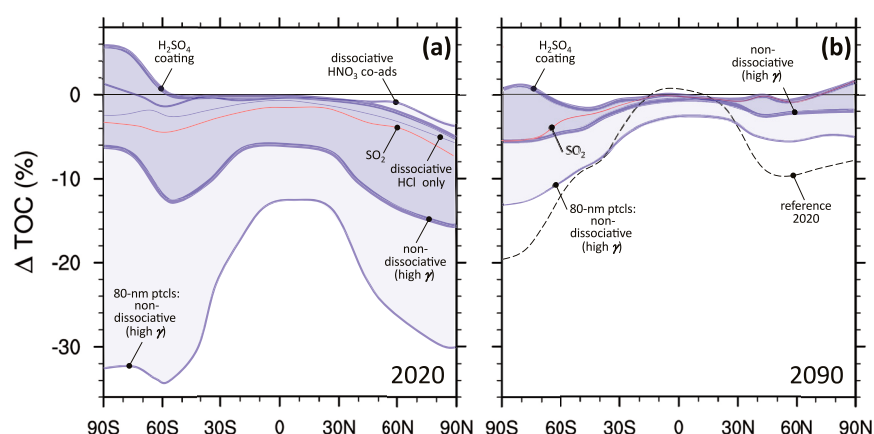


Figure 2. Zonal mean of 10 years averaged total ozone column depletion resulting from injection of 5 Mt/yr of alumina particles assuming different parameterizations of R1 (Figure 1) or alumina particles to be covered with sulfuric acid (“H₂SO₄ coating”) simulated with SOCOL-AER under (a) 2020 and (b) 2090 ozone depleting substances and greenhouse gas conditions. For comparison we also show an SO₂ injection scenario with equal injection rates as for the alumina injection scenarios (i.e., 5 Mt SO₂ per year in red).

Section 1.3). A radius of 240 nm is also close to the optimal radius for backscattering solar radiation of 215 nm reported by Dykema et al. (2016). Indeed, other simulations which account for scattering and absorption of radiation show a top-of-atmosphere (TOA) all sky radiative forcing of about -0.75 W/m^2 for 5 Mt/yr injection of 240 nm.

Scenarios were performed with different parameterizations for co-adsorption/desorption and reaction or different assumptions on the partitioning of HNO₃ and H₂SO₄ at the particle surface (blue lines in Figure 1 and Table S1 in Supporting Information S1). For comparison with sulfur-based SAI, a scenario with injections of 5 Mt of SO₂ per year (i.e., 2.5 Mt of Sulfur per year) was also run. All simulations are time-slices spanning 15 years, with climatological sea surface temperature (SST), sea ice concentrations (SIC), GHG, and ODS concentrations set to 2020 or 2090 conditions. The first 5 years of each simulation served as spin-up to equilibrate stratospheric aerosol burdens. Hence, all data shown in this study are 10-year averages. GHG and ODS concentrations were taken from SSP5-8.5 (O’Neill et al., 2015) and WMO (2018), respectively, while SST and SIC were taken from a 10-year average (2011–2020) of the Hadley data set (Kennedy et al., 2019) for 2020 conditions and CESM5-CAM1 RCP8.5 (2090–2099) for 2090 conditions (Meehl et al., 2013).

3. Results

The scenarios with injection of 5 Mt per year of particles with radius of 240 nm result in global mean stratospheric alumina burdens of about 3.7 Mt. The corresponding mean stratospheric particle residence times are about 9 months and the resulting alumina SAD is $3\text{--}5 \mu\text{m}^2/\text{cm}^3$ in the lower stratosphere (Figure S6 in Supporting Information S1). When applying the different parameterizations for co-adsorption/desorption and reaction for γ_{ClONO_2} depicted in Figure 1, the “non-dissociative high γ_{ClONO_2} ” scenario for 240-nm particles results in a TOC decrease of 9% globally, up to 16% over the poles and midlatitudes and about 6% in the tropics for present day ODS (Figure 2a). When injecting particles of a radius of 80 nm instead of 240 nm at 5 Mt/yr, the global mean aerosol burden increases to 5.2 Mt (due to reduced sedimentation). In the “non-dissociative high- γ_{ClONO_2} ” case SAD increases to $5\text{--}16 \mu\text{m}^2/\text{cm}^3$ (Text and Figure S6 in Supporting Information S1), which enhances global mean TOC depletion to more than 20% (Figure 2a).

However, most likely HNO₃ will co-adsorb on the alumina surface (Text S5 in Supporting Information S1). The scenario “ γ_{ClONO_2} with HNO₃,” which accounts for co-adsorption and dissociation of HCl and HNO₃ on the particle surface, yields no substantial ozone loss. Furthermore, gaseous H₂SO₄ can co-condense with water, and aqueous H₂SO₄ droplets can coagulate with the alumina particles. Therefore, alumina surfaces will be covered partly or fully by sulfuric acid a few weeks after injection. A full coating (core-shell configuration) is not very likely, given the contact angle of $25^\circ\text{--}38^\circ$ for macroscopic H₂SO₄-H₂O droplets on alumina surfaces (Figure S3

in Supporting Information S1). However, we analyze the sensitivity of the ozone response to alumina particles by assuming a full coating by sulfuric acid (termed “H₂SO₄ coating” in Figure 2). In this conservative scenario, the entire resulting SAD (Figure S6 in Supporting Information S1) hosts the same heterogeneous chemistry as on sulfuric acid aerosols. The impact on ozone in this scenario is small since the absolute sulfuric acid SAD increase in the extratropics is only about 20% (Figure S6 in Supporting Information S1). The increase from coated sulfuric acid SAD is partially compensated by the decrease in background sulfuric acid aerosol SAD. The TOC increase in the southern polar stratosphere is due to less PSC in the “H₂SO₄ coating” simulation, since the number density of sulfuric acid aerosols is significantly reduced, which also explains the strong positive HNO₃ anomaly over the south polar region (see Figure S8 in Supporting Information S1, ΔHNO₃). However, the microphysical interactions of alumina particles with sulfuric acid and PSC in the stratosphere is unknown and subject to large uncertainty.

To put these results into a broader context, we also performed simulations for the year 2090 with much reduced atmospheric chlorine loading using SSP5-8.5 GHG and WMO (2018) ODS boundary conditions. Under these conditions, all SAI scenarios result in substantially less ozone depletion, which also reduces the uncertainty range (gray area in Figure 2b). The reduced ozone depletion is mostly due to the much smaller chlorine loadings in these scenarios. Depletion of TOC reaches 6% in the south polar region, but only 1% in the tropics and 3% in the north polar region for the “non-dissociative high γ_{ClONO_2} ” scenario, which has the strongest depletion of TOC across all scenarios with particle radius 240 nm. The more invasive scenario using particles with 80 nm radius still results in TOC depletion of 13% over the south polar region and 3% in the tropics (Figure S9 in Supporting Information S1).

The difference between the modeled 2090 and the 2020 TOC levels (Figure 2b) is representing the effect of ozone recovery which is consistent with projections from other models (WMO, 2022). Under 2090 conditions, all scenarios result in significantly higher TOC compared with present day TOC. This means that the projected TOC changes due to future ozone recovery are still much larger than the upper limit TOC depletion in any of the SAI scenarios.

4. Summary and Conclusions

Climate intervention to cool the climate by injecting alumina particles into the lower stratosphere could have advantages over sulfur injection, such as enhanced backscattering of solar radiation and reduced stratospheric heating. However, this study reveals that alumina injection is fraught with significant uncertainties in estimating the chemical impact on the ozone layer. Using 5 Mt/yr of alumina particles with a radius of 240 nm which would result in TOA radiative forcing of about -0.75 W/m^2 , we estimate that the global mean ozone loss could be as high as 9% for 2020 conditions. This is about twice the historical peak ozone loss caused by chlorofluorocarbons and other ODS at the end of the last century (WMO, 2022).

These simulations assume that the heterogeneous reaction of ClONO₂ with HCl has a reaction probability $\gamma_{\text{ClONO}_2} \approx 0.02$, as suggested by the only available measurement (Molina et al., 1997). However, these measurements were made for conditions in exhaust plumes from solid-fuel rocket motors with HCl concentrations more than an order of magnitude higher than in the stratosphere today. We apply a Langmuir-Hinshelwood mechanism for co-adsorption/desorption and reaction to extrapolate to lower concentrations in a physically consistent manner. This shows that γ_{ClONO_2} is not well constrained due to the sparsity of experimental data, but ranges from $\gamma_{\text{ClONO}_2} = 0.019$ to $\gamma_{\text{ClONO}_2} = 0.0003$, depending on uncertain reaction rate coefficients and Langmuir constants, as well as due to the unknown effect of co-adsorption and dissociation of HNO₃ and co-condensation of H₂SO₄ on resulting Cl[−] availability. This has massive repercussions for the modeled impacts of SAI by alumina particles. An additional complication is the uncertain wettability and degree of coverage by H₂SO₄-H₂O solutions, which may further reduce impact on stratospheric ozone (see Table S1 in Supporting Information S1 for all scenarios). Other heterogeneous reactions on alumina, such as N₂O₅ hydrolysis, are presently unconstrained by experimental data, but likely play a much smaller role than R1 (Figure S10b in Supporting Information S1). Interactions with PSCs represent a further source of uncertainty.

We have identified a number of key processes as sources of uncertainty: (a) extrapolation of measured data for R1 to stratospheric trace gas concentrations, (b) lack of detailed knowledge of competitive co-adsorption and interaction with other trace gases on the surface, (c) wettability by co-condensation of H₂SO₄ and H₂O on the surface, and (d) the effect of future ODS and GHG concentration changes. The findings of this study call for investigations on heterogeneous chemistry on solid particles that incorporate present and future stratospheric

conditions in terms of temperatures, partial pressures of relevant trace gases (e.g., H_2SO_4 , ClONO_2 , N_2O_5 , HCl , and HNO_3) and relative humidity.

Data Availability Statement

The modeled data used for this study are available in the ETH research collection via Vattioni (2023a). The model code of SOCOL-AER incorporating the solid particle microphysics scheme used for data generation is available via Vattioni (2023b).

Acknowledgments

We thank Debra Weisenstein for providing the 2D-AER code, which simplified implementation of solid particles into SOCOL-AER. We also thank her and David Keith for the feedback on our work, Liviana Klein for support with the coating angle measurements and Uwe Weers with the ERDA measurements, Max Döbeli for conducting and analyzing the ERDA measurements together with Christof Vockenhuber. Gabriel Chiodo and Andrea Stenke were supported by the Swiss Science Foundation (Grant PZ00P2_180043) and Sandro Vattioni by the ETH Research Grant (Grant ETH-1719-2), as well as by the Harvard Solar Geoengineering Research Program, which also supported Frank Keutsch.

References

- Aguzzi, A., & Rossi, M. J. (2001). The kinetics of the uptake of HNO_3 on ice, solid $\text{H}_2\text{SO}_4\cdot\text{H}_2\text{O}$ and solid ternary solutions of $\text{H}_2\text{SO}_4\text{HNO}_3\cdot\text{H}_2\text{O}$ in the temperature range 180–211 K. *Physical Chemistry Chemical Physics*, 3(17), 3707–3716. <https://doi.org/10.1039/B100546O>
- Ammann, M., Cox, R. A., Crowley, J. N., Jenkin, M. E., Mellouki, A., Rossi, M. J., et al. (2013). Evaluated kinetic and photochemical data for atmospheric chemistry: Volume VI – Heterogeneous reactions with liquid substrates. *Atmospheric Chemistry and Physics*, 13(16), 8045–8228. <https://doi.org/10.5194/acp-13-8045-2013>
- Aquila, V., Garfinkel, C. I., Newman, P., Oman, L., & Waugh, D. (2014). Modifications of the quasi-biennial oscillation by a geoengineering perturbation of the stratospheric aerosol layer. *Geophysical Research Letters*, 41(5), 1738–1744. <https://doi.org/10.1002/2013GL058818>
- Arias, P. A., Bellouin, N., Coppola, E., Jones, R. G., Krinner, G., Marotzke, J., et al. (2021). Technical summary. In V. Masson-Delmotte, P. Zhai, A. Pirani, S. L. Connors, C. Péan, S. Berger, et al. (Eds.), *Climate change 2021: The physical science basis. Contribution of working group I to the sixth assessment report of the Intergovernmental Panel on Climate Change* (pp. 33–144). Cambridge University Press. <https://doi.org/10.1017/9781009157896.002>
- Bluth, G., Doiron, S., Schnetzler, C., Krueger, A., & Walter, L. (1992). Global tracking of the SO_2 clouds from the June, 1991 mount Pinatubo eruptions. *Geophysical Research Letters*, 19(2), 151–154. <https://doi.org/10.1029/91GL02792>
- Brodowsky, C., Sukhodolov, T., Feinberg, A., Höpfner, M., Peter, T., Stenke, A., & Rozanov, E. (2021). Modeling the sulfate aerosol evolution after recent moderate volcanic activity, 2008–2012. *Journal of Geophysical Research: Atmospheres*, 126(23), e2021JD035472. <https://doi.org/10.1029/2021JD035472>
- Budyko, M. (1977). *Climatic changes*. American Geophysical Union. <https://doi.org/10.1029/SP010>
- Burkholder, J., Sander, S., Abbatt, J., Barker, J., Cappa, C., Crounse, J., et al. (2020). *Chemical kinetics and photochemical data for use in atmospheric studies; evaluation number 19 (Tech. Rep.)*. Jet Propulsion Laboratory, National Aeronautics and Space.
- Carlsaw, K. S., & Peter, T. (1997). Uncertainties in reactive uptake coefficients for solid stratospheric particles-I. Surface chemistry. *Geophysical Research Letters*, 24(14), 1743–1746. <https://doi.org/10.1029/97GL01683>
- Clark, P., Shakun, J., Marcott, S., Mix, A., Eby, M., Kulp, S., et al. (2016). Consequences of twenty-first-century policy for multi-millennial climate and sea-level change. *Nature Climate Change*, 6(4), 360–369. <https://doi.org/10.1038/nclimate2923>
- Corti, T., & Krieger, U. K. (2007). Improved inverted bubble method for measuring small contact angles at crystal-solution-vapor interfaces. *Applied Optics*, 46(23), 5835–5839. <https://doi.org/10.1364/ao.46.005835>
- Crowley, J. N., Ammann, M., Cox, R. A., Hynes, R. G., Jenkin, M. E., Mellouki, A., et al. (2010). Evaluated kinetic and photochemical data for atmospheric chemistry: Volume V – Heterogeneous reactions on solid substrates. *Atmospheric Chemistry and Physics*, 10(18), 9059–9223. <https://doi.org/10.5194/acp-10-9059-2010>
- Crutzen, P. (2006). Albedo enhancement by stratospheric sulfur injections: A contribution to resolve a policy dilemma? *Climatic Change*, 77(3–4), 211–220. <https://doi.org/10.1007/s10584-006-9101-y>
- Dai, Z., Weisenstein, D. K., Keutsch, F. N., & Keith, D. W. (2020). Experimental reaction rates constrain estimates of ozone response to calcium carbonate geoengineering. *Communications Earth & Environment*, 1(1), 63. <https://doi.org/10.1038/s43247-020-00058-7>
- Dykema, J. A., Keith, D. W., & Keutsch, F. N. (2016). Improved aerosol radiative properties as a foundation for solar geoengineering risk assessment. *Geophysical Research Letters*, 43(14), 7758–7766. <https://doi.org/10.1002/2016GL069258>
- Egorova, T., Rozanov, E., Zubov, V., & Karol, I. L. (2003). Model for investigating ozone trends (MEZON). *Izvestiya Atmospheric and Oceanic Physics*, 39, 277–292.
- Feinberg, A., Sukhodolov, T., Luo, B.-P., Rozanov, E., Winkel, L. H. E., Peter, T., & Stenke, A. (2019). Improved tropospheric and stratospheric sulfur cycle in the aerosol–chemistry–climate model SOCOL-AERv2. *Geoscientific Model Development*, 12(9), 3863–3887. <https://doi.org/10.5194/gmd-12-3863-2019>
- Fernandez, M. A., Hynes, R. G., & Cox, R. A. (2005). Kinetics of ClONO_2 reactive uptake on ice surfaces at temperatures of the upper troposphere. *The Journal of Physical Chemistry A*, 109(44), 9986–9996. <https://doi.org/10.1021/jp053477b>
- Ferraro, A. J., Highwood, E. J., & Charlton-Perez, A. J. (2011). Stratospheric heating by potential geoengineering aerosols. *Geophysical Research Letters*, 38(24), L24706. <https://doi.org/10.1029/2011GL049761>
- Friedel, M., & Chiodo, G. (2022). Ozone depletion over the Arctic affects spring climate in the Northern Hemisphere. *Nature Geoscience*, 15(7), 518–519. <https://doi.org/10.1038/s41561-022-00974-7>
- Huynh, H. N., & McNeill, V. F. (2021). Heterogeneous reactivity of HCl on CaCO_3 aerosols at stratospheric temperature. *ACS Earth and Space Chemistry*, 5(8), 1896–1901. <https://doi.org/10.1021/acsearthspacechem.1c00151>
- Hynes, R. G., Fernandez, M. A., & Cox, R. A. (2002). Uptake of HNO_3 on water-ice and coadsorption of HNO_3 and HCl in the temperature range 210–235 K. *Journal of Geophysical Research*, 107(D24), AAC19-1–AAC19-11. <https://doi.org/10.1029/2001JD001557>
- Jouzel, J. (2013). A brief history of ice core science over the last 50 yr. *Climate of the Past*, 9(6), 2525–2547. <https://doi.org/10.5194/cp-9-2525-2013>
- Keith, D., & MacMartin, D. (2015). A temporary, moderate and responsive scenario for solar geoengineering. *Nature Climate Change*, 5(3), 201–206. <https://doi.org/10.1038/nclimate2493>
- Keith, D., Weisenstein, D., Dykema, J., & Keutsch, F. (2016). Stratospheric solar geoengineering without ozone loss. *Proceedings of the National Academy of Sciences of the United States of America*, 113(52), 14910–14914. <https://doi.org/10.1073/pnas.1615572113>
- Kennedy, J. J., Rayner, N., Atkinson, C., & Killick, R. (2019). An ensemble data set of sea surface temperature change from 1850: The Met Office Hadley Centre HadSST. 4.0. 0.0 data set. *Journal of Geophysical Research: Atmospheres*, 124(14), 7719–7763. <https://doi.org/10.1029/2018jd029867>

- Kottler, C., Doebeli, M., Glaes, F., & Suter, M. (2006). A spectrometer for low energy heavy ion ERDA. *Nuclear Instruments and Methods in Physics Research Section B: Beam Interactions with Materials and Atoms*, 248(1), 155–162. <https://doi.org/10.1016/j.nimb.2006.02.013>
- MacMartin, D. G., Caldeira, K., & Keith, D. W. (2014). Solar geoengineering to limit the rate of temperature change. *Philosophical Transactions of the Royal Society A: Mathematical, Physical and Engineering Sciences*, 372(2031), 20140134. <https://doi.org/10.1098/rsta.2014.0134>
- MacMartin, D. G., Ricke, K. L., & Keith, D. W. (2018). Solar geoengineering as part of an overall strategy for meeting the 1.5°C Paris target. *Philosophical Transactions of the Royal Society A: Mathematical, Physical and Engineering Sciences*, 376(2119), 20160454. <https://doi.org/10.1098/rsta.2016.0454>
- McLachlan, D., Jr., & Cox, H. M. (1975). Apparatus for measuring the contact angles at crystal-solution-vapor interfaces. *Review of Scientific Instruments*, 46(1), 80–83. <https://doi.org/10.1063/1.1134019>
- Meehl, G. A., Washington, W. M., Arblaster, J. M., Hu, A., Teng, H., Kay, J. E., et al. (2013). Climate change projections in CESM1(CAM5) compared to CCSM4. *Journal of Climate*, 26(17), 6287–6308. <https://doi.org/10.1175/JCLI-D-12-00572.1>
- Molina, M. J., Molina, L. T., Zhang, R., Meads, R. F., & Spencer, D. D. (1997). The reaction of ClONO₂ with HCl on aluminum oxide. *Geophysical Research Letters*, 24(13), 1619–1622. <https://doi.org/10.1029/97GL01560>
- NRC. (2015). *National research council, climate intervention: Reflecting sunlight to cool Earth*. The National Academies Press. <https://doi.org/10.17226/18988>
- O'Neill, B., Kriegler, E., Ebi, K., Kemp-Benedict, E., Riahi, K., Rothman, D., et al. (2015). The roads ahead: Narratives for shared socioeconomic pathways describing world futures in the 21st century. *Global Environmental Change*, 42, 169–180. <https://doi.org/10.1016/j.gloenvcha.2015.01.004>
- Pope, F., Braesicke, P., Grainger, R., Kalberer, M., Watson, I. M., Davidson, P., & Cox, R. (2012). Stratospheric aerosol particles and solar-radiation management. *Nature Climate Change*, 2(10), 713–719. <https://doi.org/10.1038/nclimate1528>
- Potter, A. E. (1978). Environmental effects of the space shuttle. *Journal of Environmental Sciences*, 21, 15–21.
- Robock, A., Jerch, K., & Bunzl, M. (2008). 20 reasons why geoengineering may be a bad idea. *Bulletin of the Atomic Scientists*, 64(2), 14–18. <https://doi.org/10.2968/064002006>
- Roekner, E., Bäuml, G., Bonaventura, L., Brokopf, R., Esch, M., Giorgetta, M., et al. (2003). The atmospheric general circulation model ECHAM 5. Part I: Model description.
- Rozanov, E. V., Schlesinger, M. E., & Zubov, V. A. (2001). The University of Illinois, Urbana-Champaign three-dimensional stratosphere-troposphere general circulation model with interactive ozone photochemistry: Fifteen-year control run climatology. *Journal of Geophysical Research*, 106(D21), 27233–27254. <https://doi.org/10.1029/2000JD000058>
- Sheng, J., Weisenstein, D. K., Luo, B., Rozanov, E., Stenke, A., Anet, J., et al. (2015). Global atmospheric sulfur budget under volcanically quiescent conditions: Aerosol-chemistry-climate model predictions and validation. *Journal of Geophysical Research: Atmospheres*, 120(1), 256–276. <https://doi.org/10.1002/2014JD021985>
- Stenke, A., Schraner, M., Rozanov, E., Egorova, T., Luo, B., & Peter, T. (2013). The SOCOL version 3.0 chemistry–climate model: Description, evaluation, and implications from an advanced transport algorithm. *Geoscientific Model Development*, 6(5), 1407–1427. <https://doi.org/10.5194/gmd-6-1407-2013>
- Tabazadeh, A., & Turco, R. P. (1993). A model for heterogeneous chemical processes on the surfaces of ice and nitric acid trihydrate particles. *Journal of Geophysical Research*, 98(D7), 12727–12740. <https://doi.org/10.1029/93JD00947>
- Thomason, L., & Peter, T. (2006). *SPARC assessment of stratospheric aerosol properties (ASAP)* (SPARC Report No. 4, WCRP-124, WMO/TD-No. 1295). Stratospheric Processes And their Role in Climate (SPARC).
- Tilmes, S., Mueller, R., & Salawitch, R. (2008). The sensitivity of polar ozone depletion to proposed geoengineering schemes. *Science*, 320(5880), 1201–1204. <https://doi.org/10.1126/science.1153966>
- Vattioni, S. (2023a). Data for: “Chemical impact of stratospheric alumina particle injection for solar radiation modification and related uncertainties” [Dataset]. ETH Zurich. <https://doi.org/10.3929/ethz-b-000626837>
- Vattioni, S. (2023b). SOCOL-AER_solid_particles [Software]. <https://doi.org/10.5281/zenodo.8398627>
- Vattioni, S., Weisenstein, D., Keith, D., Feinberg, A., Peter, T., & Stenke, A. (2019). Exploring accumulation-mode H₂SO₄ versus SO₂ stratospheric sulfate geoengineering in a sectional aerosol–chemistry–climate model. *Atmospheric Chemistry and Physics*, 19(7), 4877–4897. <https://doi.org/10.5194/acp-19-4877-2019>
- Weisenstein, D. K., Keith, D. W., & Dykema, J. A. (2015). Solar geoengineering using solid aerosol in the stratosphere. *Atmospheric Chemistry and Physics*, 15(20), 11835–11859. <https://doi.org/10.5194/acp-15-11835-2015>
- Weisenstein, D. K., Visionsi, D., Franke, H., Niemeier, U., Vattioni, S., Chiodo, G., et al. (2022). An interactive stratospheric aerosol model inter-comparison of solar geoengineering by stratospheric injection of SO₂ or accumulation-mode sulfuric acid aerosols. *Atmospheric Chemistry and Physics*, 22(5), 2955–2973. <https://doi.org/10.5194/acp-22-2955-2022>
- Weisenstein, D. K., Yue, G. K., Ko, M. K., Sze, N., Rodriguez, J. M., & Scott, C. J. (1997). A two-dimensional model of sulfur species and aerosols. *Journal of Geophysical Research*, 102(D11), 13019–13035. <https://doi.org/10.1029/97JD00901>
- Wilson, J. C., Jonsson, H. H., Brock, C. A., Toohey, D. W., Avallone, L. M., Baumgardner, D., et al. (1993). In situ observations of aerosol and chlorine monoxide after the 1991 eruption of mount Pinatubo: Effect of reactions on sulfate aerosol. *Science*, 261(5125), 1140–1143. <https://doi.org/10.1126/science.261.5125.1140>
- WMO. (2018). *Scientific assessment of ozone depletion: 2018. Global ozone research and monitoring project* Report No. 50(20). World Meteorological Organization.(p. 588).
- WMO. (2022). *Scientific assessment of ozone depletion: 2022. Global ozone research and monitoring project* Report No. 278(20). World Meteorological Organization (p. 509).
- Zimmermann, S., Kippenberger, M., Schuster, G., & Crowley, J. (2016). Adsorption isotherms for hydrogen chloride (HCl) on ice surfaces between 190 and 220 K. *Physical Chemistry Chemical Physics*, 18(20), 13799–13810. <https://doi.org/10.1039/c6cp01962e>